

Dynamics of Electron Injection in Nanocrystalline Titanium Dioxide Films Sensitized with [Ru(4,4'-dicarboxy-2,2'-bipyridine)₂(NCS)₂] by Infrared Transient Absorption

Randy J. Ellingson,^{*,†} John B. Asbury,[‡] Sue Ferrere,[†] Hirendra N. Ghosh,[‡] Julian R. Sprague,[†] Tianquan Lian,^{*,‡} and Arthur J. Nozik^{*,†}

Center for Basic Sciences, National Renewable Energy Laboratory, Golden, Colorado, 80401, and Department of Chemistry, Emory University, Atlanta, Georgia, 30322

Received: May 19, 1998; In Final Form: July 13, 1998

We have used femtosecond pump–probe spectroscopy to time resolve the injection of electrons into nanocrystalline TiO₂ film electrodes under ambient conditions following photoexcitation of the adsorbed dye, [Ru(4,4'-dicarboxy-2,2'-bipyridine)₂(NCS)₂] (N3). Pumping at one of the metal-to-ligand charge-transfer absorption peaks and probing the absorption by injected electrons in the TiO₂ at 1.52 μm and in the range of 4.1–7.0 μm, we have directly observed the arrival of electrons injected into the TiO₂ film. Our measurements indicate an instrument-limited ~50 fs upper limit on the electron injection time. We have compared the infrared transient absorption for noninjecting systems consisting of N3 in ethanol and N3 adsorbed to films of nanocrystalline Al₂O₃ and ZrO₂ and found no indication of electron injection at probe wavelengths in the mid-IR (4.1–7.0 μm).

Introduction

Extensive efforts have been directed toward understanding the photoelectrochemical properties and charge-transfer dynamics of dye-sensitized nanocrystalline semiconductor films. Such films used in photovoltaic cells have demonstrated highly efficient solar energy conversion (>10%) in recent years^{1–3} and have generated significant interest as a potential new approach to economical solar energy conversion. Dye-sensitized photoelectrochemical solar cells based on [Ru(4,4'-dicarboxy-2,2'-bipyridine)₂(NCS)₂] (N3) adsorbed to nanocrystalline TiO₂ rely on efficient charge separation at the dye-TiO₂ interface, and fast electron injection from the excited state of the adsorbed dye molecule into the TiO₂ nanoparticle. Injection must be fast to compete with processes such as relaxation and degradation of the excited dye molecule. Several groups studying the transient absorption of the excited and oxidized states of the dye in the visible and near-IR, to determine the electron injection time in the N3-sensitized TiO₂ (N3–TiO₂) and similar systems, have reported evidence for ultrafast (≤1 ps) charge separation and electron injection.^{4–9} Tachibana et al. reported transient absorption measurements at 750 nm, which were ascribed to the formation of oxidized N3 (pumped at 605 nm); analysis of the rise time of the 750 nm absorption indicated biphasic electron injection with injection times of 150 fs (instrument-limited) and 1.2 ps.⁴ Hannappel et al.⁵ measured the rise of the near-infrared absorption of conduction band electrons at 1100 nm following photoexcitation of N3 at the lower-energy metal-to-ligand charge-transfer (MLCT) absorption peak (550 nm); the near-infrared absorption signal was attributed to free or trapped electrons following injection. However, these authors believe that to obtain unambiguous results, it was necessary for these experiments to be conducted under ultrahigh vacuum (UHV) conditions. These authors also challenged the assign-

ment by Tachibana et al. of the 750 nm absorption band to oxidized N3;⁴ this challenge has been answered in turn.^{6,7} Heimer et al.⁸ used a system with 30 ps resolution to time resolve the electron injection into TiO₂ from the dye [Ru(4,4'-(COOCH₂CH₃)₂-2,2'-bipyridine)(2,2'-bipyridine)₂]²⁺; the instrument time response placed an upper limit on the injection time of ~20 ps.¹⁰ Here we present further evidence, based on time-resolved infrared (TRIR) absorption measurements, for ultrafast electron injection times (50 ± 25 fs) for the N3–TiO₂ electrode under ambient conditions. By probing the time-resolved mid-IR absorption produced by injected electrons,^{9,11} we are able to obtain unambiguous conclusions without the need for UHV. Probing in the mid-IR allows us to bypass the issue of the correct absorption spectrum for oxidized N3 and eliminate the possibility of any signal contributions from the cationic or excited states of the dye.⁹

Materials and Methods

Titanium dioxide nanoparticle colloids were prepared as previously described, using Degussa P25 TiO₂ starting material.¹² The Al₂O₃ nanoparticle colloid was prepared using a method similar to that used for TiO₂. The starting material for the alumina colloid was Degussa Aluminum Oxide C (primary particle size of 13 nm). Some adjustment of the ratio of starting material weight to distilled water volume was required for the Al₂O₃ preparation. The ZrO₂ colloid was prepared via hydrolysis of zirconium isopropoxide and heated at 220 °C using a procedure published previously for the preparation of colloidal TiO₂.¹³ Colloids were used to prepare electrodes as previously described,¹³ using a glass rod to spread the colloid over the substrate using Scotch tape as a spacer. Films were fired at 450 °C for 45 min in air. Films to be used with probe wavelengths longer than 5.5 μm were prepared on 2.0 mm thick CaF₂ substrates, both sides polished. CaF₂ substrates presented adhesion problems, but these occurred only for TiO₂, and only for films thicker than ~5 μm. Films to be used at wavelengths shorter than 5.5 μm were prepared on either *c*-cut polished

* To whom correspondence should be addressed: R.J.E., Randy_Ellingson@nrel.gov; T.L., tlian@emory.edu; A.J.N., anozik@nrel.nrel.gov.

[†] National Renewable Energy Laboratory.

[‡] Emory University.

sapphire or fluorine-doped SnO₂ conducting glass substrates. TiO₂ and ZrO₂ films were 5–8 μm thick with good transparency. Al₂O₃ films were ~15 μm thick, and showed greater scattering than the TiO₂ films. Immersion and storage of the TiO₂, Al₂O₃, and ZrO₂ films in a room-temperature ethanol solution containing 200 μM N3 and 20 mM chenodeoxycholic acid¹⁴ resulted in adsorption of the N3 dye to the porous film surface. The resulting dye-sensitized films showed an absorbance of ~1.0 at 400 and 550 nm. High-purity N3 was purchased from Solaronix (Lausanne, Switzerland).

Pump-probe measurements were made using two different laser systems. The output from a Coherent RegA 9000 regeneratively amplified titanium-doped sapphire (Ti:S) laser, operating at 10 kHz, was frequency-doubled to 400 nm and used to pump a visible optical parametric amplifier (OPA). The OPA signal wavelength, which is dependent by the parametric process on the idler wavelength, was set to 550 nm and used to pump the lower-energy MLCT absorption band for N3. Samples were probed with the OPA idler at a wavelength of 1.52 μm. The TRIR 1.52 μm absorption measurement was configured noncollinearly such that in air the beams crossed at an angle of 6°. At the point of overlap in the sample, the pump and probe beams were focused to diameters of 200 and 50 μm, respectively. The pump pulse energy was 30 nJ for an incident intensity of 95 μJ·cm⁻². Solid-state samples were in contact with air during the measurements; samples in solvent were nominally protected by purging with N₂ and sealing the cell with a rubber septum. The pump beam was chopped at 85 Hz to permit phase-sensitive detection of the probe beam, which is detected by a monochromator-mounted liquid nitrogen cooled Ge detector; the detector output was measured by a lock-in amplifier and recorded as a function of probe pulse delay.

The second system was based on a Clark-MXR 1 kHz regeneratively amplified Ti:S laser pumping an IR OPA.⁹ Difference frequency generation (DFG) between the OPA signal and idler outputs produced femtosecond pulses tunable over the range of 4.1–7.0 μm. Experiments utilizing the 1 kHz system used the frequency-doubled Ti:S output to pump the samples with 1.1 μJ, ~100 fs pulses at 400 nm. The pump and probe spot sizes were 450 and 350 μm, respectively; the corresponding pump pulse incident intensity is 700 μJ·cm⁻². Results here are for samples measured in air. The pump beam was chopped by a New Focus Model 3501 Chopper, which was driven externally by the output from the Ti:S Q-switching electronics. The relative polarization between the pump and probe beams was set at the magic angle of 54.7°. To correct for low-frequency fluctuations in the DFG power, a reference beam is split off from the DFG beam and routed around the sample. Both the probe and reference beams (parallel and vertically separated) are coupled into a CVI Digichrome 240 0.25 m monochromator. The monochromator slits were typically adjusted to pass a bandwidth of 2 cm⁻¹. The beams are then detected by separate, matched liquid nitrogen cooled HgCdTe detectors from Electro Optical Systems, Inc. Signals from the reference and probe detectors are sent to separate channels of a Stanford Research SR250 boxcar averager. The integrated outputs are digitized in a 12 bit ADC and recorded by a computer for each laser pulse.

Experimental Results

With the N3–TiO₂ sample exposed to air, transient absorption measurements using a visible pump and a visible or near-IR probe show a problematic long-lived absorption component. Hannappel et al. also observed such an accumulated signal for

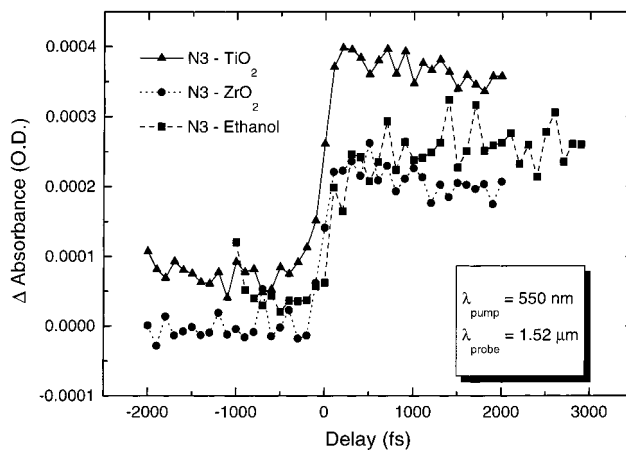


Figure 1. TRIR absorption data for 550 nm pump and 1.52 μm probe of N3–TiO₂, N3–ZrO₂, and N3–ethanol.

visible probe measurements made in a solvent environment;⁵ only when measuring solid-state samples under UHV did the accumulated signal vanish. Our initial investigations of various samples pumped at 550 nm and probed at 1.52 μm showed long-lived signals as well as signals not attributable to absorption by injected electrons. Figure 1 shows data for N3–TiO₂, N3–ZrO₂, and N3–ethanol samples. The N3–TiO₂ sample shows an ultrafast rise of absorption and subsequent initial decay, similar to that reported by Hannappel et al.⁵ However, it is clear from measurements of the N3–ZrO₂, where significant injection is not expected, and N3–ethanol, where no semiconductor is present, that other sources of transient absorption at 1.52 μm are present from either N3* or N3 photoproducts in this near-IR region. To rule out nonlinear effects such as two-photon (pump) absorption, we have verified that the absorption signal is linear with pump pulse energy. The transient signal for N3–TiO₂ may very well be dominated by the injected-electron absorption, but no clear conclusions can be drawn without well-behaved blanks to verify the absence of a signal arising from N3* or N3⁺.

Our measurements have shown that the residual signal evident at $t < 0$ (corresponding to 100 μs delay) in Figure 1 for N3–TiO₂ is reproducible. By measuring a TRIR absorption signal from directly excited electron–hole pairs for an unsensitized TiO₂ film, Hannappel et al. determined the source of the transient absorption at 1100 nm to be electrons within the TiO₂. Our transient measurement of N3–TiO₂ apparently includes both the long-lived and short-lived components, i.e., contributions from both injected-electron absorption and the as-yet undetermined long-lived effect. In contrast, the 1.52 μm transient absorption for N3–ZrO₂ shows a clear return to zero. If an N3 photodegradation product is responsible for the long-lived signal component, then apparently N3 on ZrO₂ does not photodegrade as easily as for N3–TiO₂. Possible reasons are that N3 does not inject efficiently into ZrO₂ (so that no significant cation population develops) or that any injection into ZrO₂ is more quickly followed by the back electron transfer, thereby reducing the time spent in the unstable oxidized form.

Owing to the long-lived absorption we observed when probing at 1.52 μm, we made additional transient absorption measurements at longer IR wavelengths. The samples were measured in air, and the linear absorbance at 2110 cm⁻¹ (4.74 μm) was 30 m.O.D. for the N3–TiO₂ sample and 70 m.O.D. for the N3–Al₂O₃ sample. Using the 1 kHz system, we used a pump pulse energy of 1.1 μJ at 400 nm and 100 fs pulse width to excite samples of N3–TiO₂, N3–Al₂O₃, N3–ZrO₂, and unsensitized

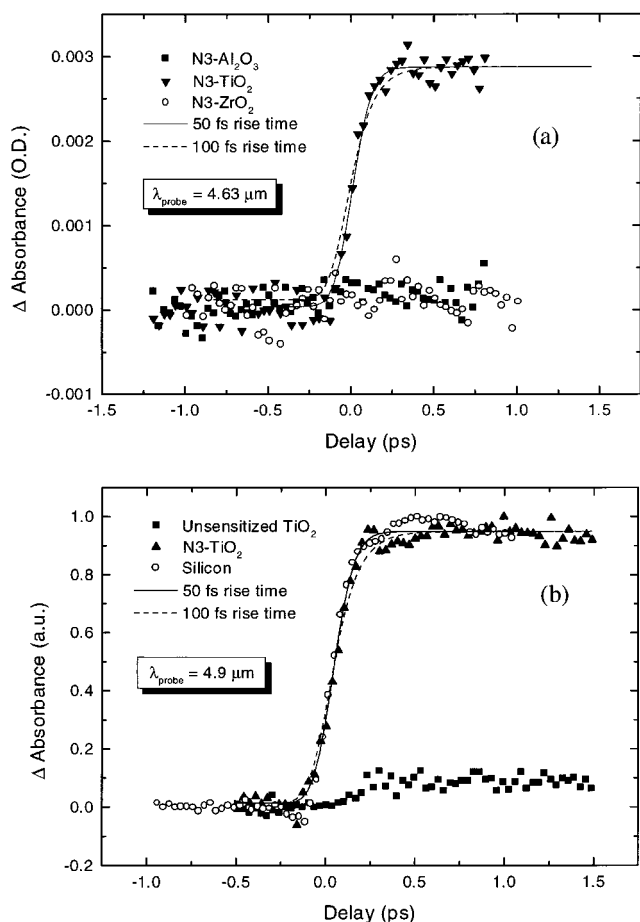


Figure 2. TRIR absorption data for probe wavelengths of (a) 4.63 μm and (b) 4.9 μm following photoexcitation by 400 nm, 100 fs pulses. As seen in (a), neither N3-Al₂O₃ nor N3-ZrO₂ show evidence of injected-electron absorption. The system response function from free-carrier absorption in silicon shown in (b) is seen to match very closely the rise of the absorption signal for N3-TiO₂; unsensitized TiO₂ shows a small absorption due to carriers photoexcited directly within the electrode. The rise times indicate an injection time \sim 50 fs.

TiO₂. Probing the resultant absorption at 4.63 and 4.9 μm , we find no transient absorbance for either the N3-Al₂O₃ or N3-ZrO₂ samples, and only a small absorbance for the unsensitized TiO₂. N3-TiO₂ shows a transient absorbance maximum of \sim 3 mO.D. at 4.63 μm and \sim 6 mO.D. for 4.9 μm . Results are shown in Figure 2. The transient mid-IR signals can be well fit by a single-exponential rise convoluted with the instrument response function. The best fits yield time constants of 50 ± 25 fs, as shown by the solid lines in Figure 2a,b. The rise time of 100 fs does not produce as satisfactory a fit of the data, as shown by the dashed line. The instrument response function was determined in a thin silicon wafer right before or after a kinetics scan at each wavelength. A typical response in silicon is shown in Figure 2b; this signal can be well-represented by the integration of a Gaussian function with fwhm of 185 fs. The transient absorbance for the unsensitized TiO₂ is \sim 0.6 mO.D., \sim 10% of the absorbance for N3-TiO₂ at 4.9 μm . These results show conclusive and direct evidence of the arrival of electrons within the TiO₂ following photoexcitation of adsorbed molecules of N3.

As shown in Figure 3, when probing at 6.6 μm we obtain similar results showing electron injection for N3-TiO₂, no injection for N3-Al₂O₃, and slight IR absorption for unsensitized TiO₂. In addition, the data shows a fast initial decay following the rise; this decay occurs on a \sim 50 fs time scale.

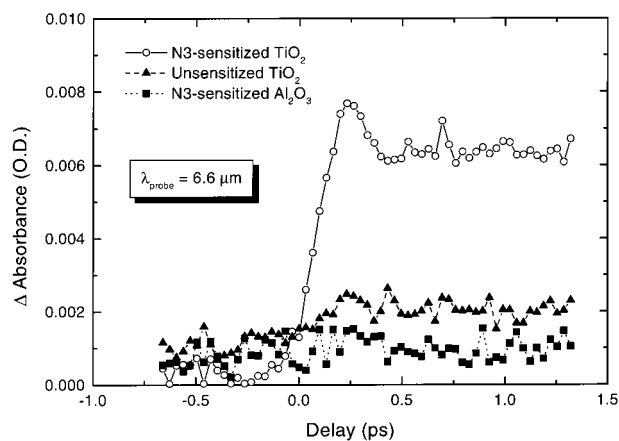


Figure 3. TRIR absorption of a 6.6 μm probe for N3-TiO₂, N3-Al₂O₃, and unsensitized TiO₂ following photoexcitation by 400 nm, 100 fs pulses. The fast (\sim 50 fs) rise of absorption for N3-TiO₂ is followed by an equally fast initial decay. The source of this decay has not been decisively assigned, though it is believed to be due to cooling or trapping of the injected electrons.

The origin of the initial decay is not determined but is consistent with either the cooling or trapping of the injected electrons. The free electron absorption cross section is proportional to the density of states, and relaxation of electrons toward the conduction band minimum is expected to result in reduced IR absorption. Trapping of electrons could also result in a reduced IR absorption. Our preliminary measurement of the spectral dependence of the IR absorption indicates an absorbance that increases with probe wavelength.

Discussion

Using TRIR absorption spectroscopy, we have measured the electron injection time for N3-TiO₂. Pumping samples of N3-ethanol, N3-TiO₂, N3-Al₂O₃, and N3-ZrO₂ at 400 or 550 nm, we probed the absorption by injected electrons using infrared femtosecond pulses at 1.52 μm and also in the range of 4.1–7.0 μm . Our results from the 1.52 μm TRIR experiments show the presence of long-lived absorption, as well as absorption by N3-ethanol and N3-ZrO₂. Any injection from N3-ZrO₂ is likely quite inefficient, and N3-ethanol provides no free or trapped electrons; therefore, the absorption signals for these samples could be due to products of the photodegradation of N3 or possibly to lower-lying N3 excited-state absorption. Hannappel et al.⁵ did not present transient absorption data for a noninjecting electrode such as N3-ZrO₂ or N3-Al₂O₃. They did report that measurements of the visible transient absorption made in a solvent or air environment exhibited an accumulated signal, which they attributed to “side reactions”. To overcome this spurious accumulated signal, they made all solid-state measurements in a UHV environment. We have found that probing further into the IR, in the 4.1–7.0 μm range, simplifies measurement of the TRIR absorption by injected electrons by eliminating the requirement of the UHV apparatus; we observed no accumulated or long-lived absorption components in this wavelength range. In addition, our results indicate that we eliminate the possibility of any contribution to the IR absorption signal arising from the dye excited or cationic states; the former could arise from noninjecting dye molecules. Analysis of our transient absorption data for probe wavelengths of 4.63, 4.9, and 6.6 μm shows an instrument-limited electron injection time for N3-TiO₂ of \sim 50 fs. For Al₂O₃ with a band gap of \sim 10 eV, and ZrO₂ with a band gap of 5 eV,^{15–18} the conduction band edge is expected to lie too far negative to allow

injection from N3*. As expected, our TRIR absorption measurements indicate that while N3–TiO₂ produces an IR-absorbing electron population within the semiconductor, no such absorption is present for the noninjecting N3–Al₂O₃ and N3–ZrO₂ samples. The broad IR absorption of N3–TiO₂ could be due to free electrons, trapped electrons, or both. Data taken at 6.6 μm suggests a cooling or trapping of the injected electrons on the ~50 fs time scale. Efforts to measure the time-resolved injected-electron IR absorption spectrum for N3–TiO₂ are underway.

As further evidence of electron injection from N3* into TiO₂, we have measured the ultrafast transient infrared absorption for the C–N stretch of the thiocyanate ligand. N3 in ethanol (without any semiconductor present) shows a depletion of the N3 ground-state C–N stretch bands at ~2115 and ~2140 cm⁻¹ and an absorption of the N3* C–N stretch bands at ~2035 and ~2075 cm⁻¹. Measurement of the N3–Al₂O₃ sample also showed both the depletion at ~2120 cm⁻¹ and the absorption at 2050 cm⁻¹; the dual bands are not resolved for N3–Al₂O₃. For these noninjecting samples (N3–ethanol and N3–Al₂O₃), the rise of both the depletion and absorption signals is instrument-limited. A similar C–N stretch measurement for the N3–TiO₂ sample is less straightforward. Although we expect the presence of the C–N stretch depletion of the N3 ground state for N3–TiO₂, the IR absorption by the injected electrons within the TiO₂ dominates the signal owing to its larger cross section. Complete results of these spectral measurements will be presented elsewhere.

Conclusions

We have measured the transient absorption of near- and mid-IR probe light by electrons injected into TiO₂ film electrodes from photoexcited sensitizing N3 molecules under ambient conditions. Our analysis indicates an upper limit on the electron injection time of about 50 fs. This injection time agrees with previous measurements made in the near-IR under UHV conditions and provides further direct evidence of the ultrafast injection process in this dye-sensitized semiconductor system. Probing the electron absorption in the mid-IR allows us to time resolve the electron injection without the presence of undesirable long-lived signals and without the need to use UHV conditions that are required for measurements made in the near-IR (1.1 and 1.52 μm). We are currently investigating the spectral dependence of the time-resolved injected-electron IR absor-

bance. A reliable measurement of the spectral dependence may reveal the dominant phonon–photon scattering process involved in the IR absorption; additionally, knowledge of intra- and intersubband cooling and trapping dynamics within the nanocrystalline TiO₂ may be gained.

Acknowledgment. R.J.E., S.F., J.R.S., and A.J.N. of NREL were supported by the U.S. Department of Energy, Office of Energy Research, Division of Chemical Sciences. J.A., H.N.G., and T.L. of EU were supported by the Petroleum Research Fund (administered by the American Chemical Society), the Emory University Research Committee, and the National Science Foundation CAREER award under Grant 9733796. We thank Brian Fluegel for his assistance with the 1.52 μm transient absorption measurements.

References and Notes

- (1) O'Regan, B.; Grätzel, M. *Nature* **1991**, *353*, 737.
- (2) Nazeeruddin, M. K.; Pechy, P.; Grätzel, M. *Chem. Commun.* **1997**, 1705.
- (3) Grätzel, M. Photoelectrochemical Solar Energy Conversion by Dye Sensitization. in *Future Generation Photovoltaic Technologies*; McConnell, R. D., Ed.; A.I.P. Conference Proceedings, 404; American Institute of Physics: Woodbury, NY, 1997.
- (4) Tachibana, Y.; Moser, J. E.; Grätzel, M.; Klug, D. R.; Durrant, J. R. *J. Phys. Chem.* **1996**, *100*, 20056.
- (5) Hannappel, T.; Burfeindt, B.; Storck, W.; Willig, F. *J. Phys. Chem. B* **1997**, *101*, 6799.
- (6) Moser, J. E.; Nourkakis, D.; Bach, U.; Tachibana, Y.; Klug, D. R.; Durrant, J. R.; Humphry-Baker, R.; Grätzel, M. *J. Phys. Chem. B* **1998**, *102*, 3649.
- (7) Hannappel, T.; Zimmermann, C.; Meissner, B.; Burfeindt, B.; Storck, W.; Willig, F. *J. Phys. Chem. B* **1998**, *102*, 3651.
- (8) Heimer, T. A.; Heilweil, E. J. *J. Phys. Chem. B* **1997**, *101*, 10990.
- (9) Ghosh, H. N.; Asbury, J. B.; Lian, T. *J. Phys. Chem. B*, in press.
- (10) A more recent measurement with improved time resolution in the subpicosecond range revealed an injection time of ~500 fs (Heilweil, E. J., private communication).
- (11) Pankove, J. I. *Optical Processes in Semiconductors*; Dover: New York, 1975.
- (12) Nazeeruddin, M. K.; Kay, A.; Rodicio, I.; Humphry-Baker, R.; Müller, E.; Liska, P.; Vlachopoulos, N.; Grätzel, M. *J. Am. Chem. Soc.* **1993**, *115*, 6382.
- (13) Zaban, A.; Ferrere, S.; Sprague, J.; Gregg, B. A. *J. Phys. Chem.* **1997**, *101*, 55.
- (14) Kay, A.; Grätzel, M. *J. Phys. Chem.* **1993**, *97*, 6272.
- (15) Bendoraitis, J. G.; Salomon, R. E. *J. Phys. Chem.* **1965**, *69*, 3666.
- (16) Clechet, P.; Martin, J.; Oliver, R.; Vallouy, C. *C. R. Acad. Sci. C* **1976**, *282*, 887.
- (17) Kung, H. H.; Jarrett, H. S.; Sleight, A. W.; Ferretti, A. *J. Appl. Phys.* **1977**, *48*, 2463.
- (18) Heimer, T. A.; Meyer, G. J. *J. Lumin.* **1996**, *70*, 468.